A Comprehensive Study of Discontinuities in Chirowaveguides

Thomas X. Wu, *Senior Member, IEEE,* and Dwight L. Jaggard, *Fellow, IEEE*

***Abstract*—We provide a comprehensive study of two- and three-dimensional discontinuities in chirowaveguides. The multimode coupled-mode method is an effective numerical approach to analyze this problem. After obtaining the coupled-mode equations, we diagonalize the coupling matrix to obtain a multimode scattering matrix rather than the usual two-mode approximation. We calculate the scattering properties of coaxial waveguides partially filled with lossy chiral media. Excellent agreement is observed between our results and those obtained by the mode-matching method. We also compare our results in the achiral case for dielectric material partially filled rectangular waveguide with experimental data and results obtained by the mode-matching method. Excellent agreement is again found. Based on our analysis, numerical and analytical results are displayed to provide physical insight into the problem. First, we discuss the effects of the chirality admittance on scattering properties and find that the sensitivity of the scattering parameters to chirality admittance increases as the chirality admittance increases. Second, we find the dielectric constant has a great influence on the scattering parameters. Third, we find the relative influence of height and width of chiral obstacles in rectangular waveguides.**

***Index Terms*—Chiral material, chirowaveguide, coupled-mode method, discontinuity.**

I. Introduction

DURING THE past decade, attention has been focused on electromagnetic chirality [1]–[3] and its application to microwave, millimeter-wave, and optical waveguided structures. The concept of chirowaveguides was introduced by Engheta and Pelet [4], [5], and the characteristics of uniform chirowaveguides have been extensively investigated [4]–[10]. As a further step toward the design of novel devices and circuits, the analysis of various discontinuities in chirowaveguides is important. Recently, two-dimensional (2-D) discontinuities in chirowaveguides were studied by several researchers. For example, Mariotte and Engheta analyzed the reflection and transmission of guided electromagnetic waves at a chiral slab in a parallel-plate waveguide [11], [12], Wu and Mariotte analyzed a partially filled chiral media coaxial waveguide [13], Busse and Jacob analyzed lossy chiral slabs in circular waveguides [14], and the authors analyzed open planar chirowaveguides with discontinuities [15], [16]. However, to our knowledge, three-dimensional (3-D) discontinuities in chirowaveguides have not been analyzed to date.

In this paper, we provide a comprehensive study of discontinuities in chirowaveguides. It is also the first study of 3-D discontinuities in chirowaveguides. We focus on the effects of discontinuities for metallic waveguide partially filled with chiral media. Our procedure is to treat the discontinuity problem by a multimode coupled-mode method. We use the eigenfunctions of a hollow metallic waveguide as basis functions to expand the fields in the chiral media partially filled region and then insert those expressions together with the chiral constitutive relations into Maxwell's equations. Using the orthogonality relations of the metallic waveguide, we obtain a set of multimode coupled-mode equations. Approximate coupled-mode theory has been used in the analysis of mode-coupling effects of chirowaveguides and chiral periodic structures [17]–[22]. Although the multimode coupled-mode method has been used to analyze the eigenvalue problem of straight chirowaveguides and bianisotropic waveguides [23], [24], we use the multimode coupled-mode equations to provide a useful numerical solution for discontinuities rather than straight waveguides in this paper. In our discontinuity analysis, we consider the influence of higher order modes rather than using only two modes in approximate coupled-mode theory, which considers only the forward and backward dominant or/and first higher order modes. Therefore, our method is useful for discontinuities with significant geometric variations.

In our analysis, we diagonalize the coupling matrix whose eigenvalues and eigenfunctions are associated with the eigenvalues and eigenfunctions of the partially filled chirowaveguide. After matrix manipulations, we obtain a multimode scattering matrix for the entire structure. From these results, we find the scattering properties of the discontinuities.

Based on the above analysis, we solve this problem numerically. We first analyze a lossy chiral media partially filled coaxial waveguide and compare our results with those obtained by the mode-matching method [13] and excellent agreement is found. We also validate our numerical analysis using the achiral case for dielectric material partially filled rectangular waveguide with experimental data [25] and results obtained by the mode-matching method proposed in [26]. Excellent agreement is again found. Based on our analysis, numerical and analytical results are displayed to provide physical insight into the problem. First, we discuss the effects of the chirality admittance on scattering properties and find that the sensitivity of the scattering parameters to chirality admittance increases as the chirality admittance increases. Second, we find the

Manuscript received July 4, 2001. This work was supported in part by the North Atlantic Treaty Organization under Collaborative Research Grant 930923, by the Complex Media Laboratory, University of Pennsylvania, and by the School of Electrical Engineering and Computer Science, University of Central Florida.

T. X. Wu is with the School of Electrical Engineering and Computer Science, University of Central Florida, Orlando, FL 32816 USA.

D. L. Jaggard is with the Complex Media Laboratory, Moore School of Electrical Engineering, University of Pennsylvania, Philadelphia, PA 19104-6390 USA.

Digital Object Identifier 10.1109/TMTT.2002.803426.

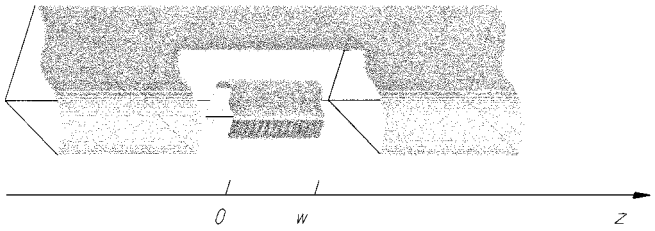

Fig. 1. Configuration of a chiral media partially filled waveguide with arbitrary cross section.

dielectric constant has a great influence on the scattering parameters. Third, we find the relative influence of height and width of chiral obstacles in rectangular waveguides. All the results are explained on the basis of underlying physics.

II. Analysis

As an example of the discontinuity problem, let us consider a metallic waveguide with arbitrary cross section partially filled with chiral media, as shown in Fig. 1.

For the chiral media, the constitutive relations for time–harmonic fields ($e^{j\omega t}$) can be written as [1]–[3]

$$\begin{cases} \mathbf{D} = \epsilon \mathbf{E} - j\xi_c \mathbf{B} \\ \mathbf{H} = \mathbf{B}/\mu - j\xi_c \mathbf{E} \end{cases} \tag{1}$$

where ξ_c is the chirality admittance, ϵ is the permittivity, and μ is the permeability.

Substituting the above constitutive relations into Maxwell's curl equations, we obtain

$$\begin{cases} \nabla \times \mathbf{E} = -j\omega\mu\mathbf{H} + \omega\kappa\sqrt{\mu\epsilon_c}\,\mathbf{E} \\ \nabla \times \mathbf{H} = j\omega\epsilon_c\mathbf{E} + \omega\kappa\sqrt{\mu\epsilon_c}\,\mathbf{H} \end{cases} \tag{2}$$

where $\epsilon_c = \epsilon + \mu\xi_c^2$, and κ is a dimensionless and normalized quantity, called the chirality parameter, defined as $\kappa = \xi_c\sqrt{\mu/\epsilon_c}$. In homogeneous media, the solutions of (2) are right circularly polarized (RCP) and left circularly polarized (LCP) eigenwaves. The wavenumbers for the two eigenwaves are

$$k_\pm = \pm\omega\mu\xi_c + \omega\sqrt{\mu\epsilon + \mu^2\xi_c^2} \tag{3}$$

where the plus ($+$) and minus ($-$) subscripts denote the RCP wave and LCP wave, respectively.

The electric and magnetic fields in (2) can be expressed by the summation of transverse and longitudinal fields as

$$\begin{cases} \mathbf{E} = \mathbf{E}_t + \mathbf{i}_z E_z \\ \mathbf{H} = \mathbf{H}_t + \mathbf{i}_z H_z. \end{cases} \tag{4}$$

Cross multiplying (2) by $\mathbf{i}_z$, we have

$$\begin{cases} \dfrac{\partial \mathbf{E}_t}{\partial z} = \nabla_t E_z + K_{11}(\mathbf{E}_t \times \mathbf{i}_z) + K_{12}(\mathbf{H}_t \times \mathbf{i}_z) \\ \dfrac{\partial \mathbf{H}_t}{\partial z} = \nabla_t H_z + K_{21}(\mathbf{E}_t \times \mathbf{i}_z) + K_{22}(\mathbf{H}_t \times \mathbf{i}_z) \end{cases} \tag{5}$$

where

$$\mathbf{K} = \begin{bmatrix} K_{11} & K_{12} \\ K_{21} & K_{22} \end{bmatrix} = \begin{bmatrix} \omega\mu\xi_c & -j\omega\mu \\ j\omega\epsilon_c & \omega\mu\xi_c \end{bmatrix}. \tag{6}$$

On the other hand, scalar multiplying (2) by $\mathbf{i}_z$, we obtain

$$\begin{bmatrix} E_z \\ H_z \end{bmatrix} = \mathbf{K}^{-1} \begin{bmatrix} \nabla_t \cdot (\mathbf{E}_t \times \mathbf{i}_z) \\ \nabla_t \cdot (\mathbf{H}_t \times \mathbf{i}_z) \end{bmatrix} \tag{7}$$

where $\mathbf{K}^{-1}$ is the matrix inversion of $\mathbf{K}$ whose elements are

$$\mathbf{K}^{-1} = \begin{bmatrix} \hat{K}_{11} & \hat{K}_{12} \\ \hat{K}_{21} & \hat{K}_{22} \end{bmatrix} = \frac{-1}{k_+ k_-} \begin{bmatrix} \omega\mu\xi_c & j\omega\mu \\ -j\omega\epsilon_c & \omega\mu\xi_c \end{bmatrix}. \tag{8}$$

Substituting (7) into (5), we obtain

$$\begin{cases} \dfrac{\partial \mathbf{E}_t}{\partial z} = \nabla\big[\hat{K}_{11}\nabla_t \cdot (\mathbf{E}_t \times \mathbf{i}_z) + \hat{K}_{12}\nabla_t \cdot (\mathbf{H}_t \times \mathbf{i}_z)\big] \\ \qquad\qquad + K_{11}(\mathbf{E}_t \times \mathbf{i}_z) + K_{12}(\mathbf{H}_t \times \mathbf{i}_z) \\ \dfrac{\partial \mathbf{H}_t}{\partial z} = \nabla\big[\hat{K}_{21}\nabla_t \cdot (\mathbf{E}_t \times \mathbf{i}_z) + \hat{K}_{22}\nabla_t \cdot (\mathbf{H}_t \times \mathbf{i}_z)\big] \\ \qquad\qquad + K_{21}(\mathbf{E}_t \times \mathbf{i}_z) + K_{22}(\mathbf{H}_t \times \mathbf{i}_z). \end{cases} \tag{9}$$

In our analysis, we expand the transverse electromagnetic fields in the chiral media partially filled region by the summation of the eigenfunctions of the hollow metallic waveguide as

$$\begin{cases} \mathbf{E}_t = \displaystyle\sum_k \sqrt{Z'_k}\left(A'^{+}_k + A'^{-}_k\right)\mathbf{e}'_k \\ \qquad\quad + \displaystyle\sum_k \sqrt{Z''_k}\left(A''^{+}_k + A''^{-}_k\right)\mathbf{e}''_k \\ \mathbf{H}_t = \displaystyle\sum_k \sqrt{Y'_k}\left(A'^{+}_k - A'^{-}_k\right)\mathbf{h}'_k \\ \qquad\quad + \displaystyle\sum_k \sqrt{Y''_k}\left(A''^{+}_k - A''^{-}_k\right)\mathbf{h}''_k \end{cases} \tag{10}$$

where quantities with a single and double prime denote the TE and TM modes, respectively. In our notation, quantities without a single or double prime may denote either TE or TM modes. The superscript "$+$" and "$-$" denote the modes propagating along the positive z-direction and negative z-direction, respectively. Here, $\mathbf{e}_k$ and $\mathbf{h}_k$ are eigenfunctions in the cross section of metallic waveguide and Z_{ck} $(=1/Y_{ck})$ are the characteristic impedances. They are given by

$$\mathbf{e}'_{\mathbf{tk}} = \mathbf{i_z} \times \nabla_t \phi'_k$$
$$\mathbf{h}'_{\mathbf{tk}} = -\nabla_t \phi'_k \tag{11}$$
$$\mathbf{e}''_{\mathbf{tk}} = \nabla_t \phi''_k$$
$$\mathbf{h}''_{\mathbf{tk}} = \mathbf{i_z} \times \nabla_t \phi''_k \tag{12}$$
$$Z_{ck} = \frac{1}{Y_{ck}} = \begin{cases} k''_{zk}/\omega\epsilon_0, & \text{for TM modes} \\ \omega\mu_0/k'_{zk}, & \text{for TE modes.} \end{cases} \tag{13}$$

Equation (10) is the Fourier series expansions of the fields in partially filled chiral media region using the eigenfunctions of hollow waveguide as basis functions. Substituting (10) into

(9) and making use of the orthogonality relations of the metallic waveguide [27], we obtain a set of coupled-mode equations

$$\begin{cases} \dfrac{d\mathbf{A}'^{+}}{dz} = \mathbf{P}_{11}\mathbf{A}'^{+} + \mathbf{P}_{12}\mathbf{A}''^{+} + \mathbf{P}_{13}\mathbf{A}'^{-} + \mathbf{P}_{14}\mathbf{A}''^{-} \\ \dfrac{d\mathbf{A}''^{+}}{dz} = \mathbf{P}_{21}\mathbf{A}'^{+} + \mathbf{P}_{22}\mathbf{A}''^{+} + \mathbf{P}_{23}\mathbf{A}'^{-} + \mathbf{P}_{24}\mathbf{A}''^{-} \\ \dfrac{d\mathbf{A}'^{-}}{dz} = \mathbf{P}_{31}\mathbf{A}'^{+} + \mathbf{P}_{32}\mathbf{A}''^{+} + \mathbf{P}_{33}\mathbf{A}'^{-} + \mathbf{P}_{34}\mathbf{A}''^{-} \\ \dfrac{d\mathbf{A}''^{-}}{dz} = \mathbf{P}_{41}\mathbf{A}'^{+} + \mathbf{P}_{42}\mathbf{A}''^{+} + \mathbf{P}_{43}\mathbf{A}'^{-} + \mathbf{P}_{44}\mathbf{A}''^{-} \end{cases} \tag{14}$$

where

$$\begin{cases} \mathbf{A}'^{+} = \left(A_1'^{+}, A_2'^{+}, \ldots\right)^T \\ \mathbf{A}'^{-} = \left(A_1'^{-}, A_2'^{-}, \ldots\right)^T \\ \mathbf{A}''^{+} = \left(A_1''^{+}, A_2''^{+}, \ldots\right)^T \\ \mathbf{A}''^{-} = \left(A_1''^{-}, A_2''^{-}, \ldots\right)^T \end{cases} \tag{15}$$

$$\begin{cases} \mathbf{P}_{11} = (\mathbf{M}_1 + \mathbf{F}_1 + \mathbf{G}_1 + \mathbf{N}_1)/2 \\ \mathbf{P}_{13} = (\mathbf{M}_1 - \mathbf{F}_1 + \mathbf{G}_1 - \mathbf{N}_1)/2 \\ \mathbf{P}_{31} = (\mathbf{M}_1 + \mathbf{F}_1 - \mathbf{G}_1 - \mathbf{N}_1)/2 \\ \mathbf{P}_{33} = (\mathbf{M}_1 - \mathbf{F}_1 - \mathbf{G}_1 + \mathbf{N}_1)/2 \\ \mathbf{P}_{12} = (\mathbf{M}_2 + \mathbf{F}_2 + \mathbf{G}_2 + \mathbf{N}_2)/2 \\ \mathbf{P}_{14} = (\mathbf{M}_2 - \mathbf{F}_2 + \mathbf{G}_2 - \mathbf{N}_2)/2 \\ \mathbf{P}_{32} = (\mathbf{M}_2 + \mathbf{F}_2 - \mathbf{G}_2 - \mathbf{N}_2)/2 \\ \mathbf{P}_{34} = (\mathbf{M}_2 - \mathbf{F}_2 - \mathbf{G}_2 + \mathbf{N}_2)/2 \\ \mathbf{P}_{21} = (\mathbf{M}_3 + \mathbf{F}_3 + \mathbf{G}_3 + \mathbf{N}_3)/2 \\ \mathbf{P}_{23} = (\mathbf{M}_3 - \mathbf{F}_3 + \mathbf{G}_3 - \mathbf{N}_3)/2 \\ \mathbf{P}_{41} = (\mathbf{M}_3 + \mathbf{F}_3 - \mathbf{G}_3 - \mathbf{N}_3)/2 \\ \mathbf{P}_{43} = (\mathbf{M}_3 - \mathbf{F}_3 - \mathbf{G}_3 + \mathbf{N}_3)/2 \\ \mathbf{P}_{22} = (\mathbf{M}_4 + \mathbf{F}_4 + \mathbf{G}_4 + \mathbf{N}_4)/2 \\ \mathbf{P}_{24} = (\mathbf{M}_4 - \mathbf{F}_4 + \mathbf{G}_4 - \mathbf{N}_4)/2 \\ \mathbf{P}_{42} = (\mathbf{M}_4 + \mathbf{F}_4 - \mathbf{G}_4 - \mathbf{N}_4)/2 \\ \mathbf{P}_{44} = (\mathbf{M}_4 - \mathbf{F}_4 - \mathbf{G}_4 + \mathbf{N}_4)/2 \end{cases} \tag{16}$$

and the elements of the matrices on the right-hand side of (16) are

$$\begin{cases} \{\mathbf{M}_1\}_{ik} = -Y_{ci}'Z_{ck}' \displaystyle\iint_S K_{11}\mathbf{e}'_i \cdot \mathbf{h}'_k \, dS \\ \{\mathbf{M}_2\}_{ik} = -Y_{ci}'Z_{ck}'' \displaystyle\iint_S K_{11}\mathbf{e}'_i \cdot \mathbf{h}''_k \, dS \\ \{\mathbf{M}_3\}_{ik} = -Y_{ci}''Z_{ck}' \left[\displaystyle\iint_S K_{11}\mathbf{e}''_i \cdot \mathbf{h}'_k \, dS - k_{ci}''^2 k_{ck}'^2 \iint_S \hat{K}_{11}\phi''_i\phi'_k \, dS \right] \\ \{\mathbf{M}_4\}_{ik} = -Y_{ci}''Z_{ck}'' \displaystyle\iint_S K_{11}\mathbf{e}''_i \cdot \mathbf{h}''_k \, dS \end{cases} \tag{17}$$

$$\begin{cases} \{\mathbf{F}_1\}_{ik} = Y_{ci}'Y_{ck}' \displaystyle\iint_S K_{12}\mathbf{e}'_i \cdot \mathbf{e}'_k \, dS \\ \{\mathbf{F}_2\}_{ik} = Y_{ci}'Y_{ck}'' \displaystyle\iint_S K_{12}\mathbf{e}'_i \cdot \mathbf{e}''_k \, dS \\ \{\mathbf{F}_3\}_{ik} = Y_{ci}''Y_{ck}' \displaystyle\iint_S K_{12}\mathbf{e}''_i \cdot \mathbf{e}'_k \, dS \\ \{\mathbf{F}_4\}_{ik} = Y_{ci}''Y_{ck}'' \left[\displaystyle\iint_S K_{12}\mathbf{e}''_i \cdot \mathbf{e}''_k \, dS - k_{ci}''^2 k_{ck}''^2 \iint_S \hat{K}_{12}\phi''_i\phi''_k \, dS \right] \end{cases} \tag{18}$$

$$\begin{cases} \{\mathbf{G}_1\}_{ik} = -Z_{ci}'Z_{ck}' \left[\displaystyle\iint_S K_{21}\mathbf{h}'_i \cdot \mathbf{h}'_k \, dS - k_{ci}'^2 k_{ck}'^2 \iint_S \hat{K}_{21}\phi'_i\phi'_k \, dS \right] \\ \{\mathbf{G}_2\}_{ik} = -Z_{ci}'Z_{ck}'' \displaystyle\iint_S K_{21}\mathbf{h}'_i \cdot \mathbf{h}''_k \, dS \\ \{\mathbf{G}_3\}_{ik} = -Z_{ci}''Z_{ck}' \displaystyle\iint_S K_{21}\mathbf{h}''_i \cdot \mathbf{h}'_k \, dS \\ \{\mathbf{G}_4\}_{ik} = -Z_{ci}''Z_{ck}'' \displaystyle\iint_S K_{21}\mathbf{h}''_i \cdot \mathbf{h}''_k \, dS \end{cases} \tag{19}$$

$$\begin{cases} \{\mathbf{N}_1\}_{ik} = Z_{ci}'Y_{ck}' \displaystyle\iint_S K_{22}\mathbf{h}'_i \cdot \mathbf{e}'_k \, dS \\ \{\mathbf{N}_2\}_{ik} = Z_{ci}'Y_{ck}'' \left[\displaystyle\iint_S K_{22}\mathbf{h}'_i \cdot \mathbf{e}''_k \, dS - k_{ci}'^2 k_{ck}''^2 \iint_S \hat{K}_{22}\phi'_i\phi''_k \, dS \right] \\ \{\mathbf{N}_3\}_{ik} = Z_{ci}''Y_{ck}' \displaystyle\iint_S K_{22}\mathbf{h}''_i \cdot \mathbf{e}'_k \, dS \\ \{\mathbf{N}_4\}_{ik} = Z_{ci}''Y_{ck}'' \displaystyle\iint_S K_{22}\mathbf{h}''_i \cdot \mathbf{e}''_k \, dS. \end{cases} \tag{20}$$

Equation (14) can be expressed in the following compact form as:

$$\frac{d\mathbf{A}}{dz} = \mathbf{P}\mathbf{A} \tag{21}$$

where

$$\mathbf{A} = \begin{bmatrix} \mathbf{A}'^{+} \\ \mathbf{A}''^{+} \\ \mathbf{A}'^{-} \\ \mathbf{A}''^{-} \end{bmatrix} \tag{22}$$

and

$$\mathbf{P} = \begin{bmatrix} \mathbf{P}_{11} & \mathbf{P}_{12} & \mathbf{P}_{13} & \mathbf{P}_{14} \\ \mathbf{P}_{21} & \mathbf{P}_{22} & \mathbf{P}_{23} & \mathbf{P}_{24} \\ \mathbf{P}_{31} & \mathbf{P}_{32} & \mathbf{P}_{33} & \mathbf{P}_{34} \\ \mathbf{P}_{41} & \mathbf{P}_{42} & \mathbf{P}_{43} & \mathbf{P}_{44} \end{bmatrix}. \tag{23}$$

Uncoupling the coupled differential equation set (21) is possible by a linear transformation upon the amplitudes. In this

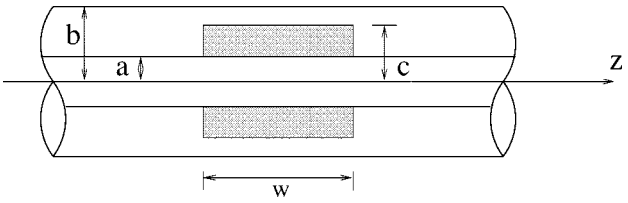

Fig. 2. Configuration of a chiral media partially filled coaxial waveguide.

case, the transformation is approached numerically. The coupling matrix $\mathbf{P}$ can be transformed into a diagonal matrix $\mathbf{K_z}$ by means of a transformation matrix $\mathbf{T}$ as follows:

$$\mathbf{TPT}^{-1} = -j\mathbf{K_z} \tag{24}$$

where

$$\mathbf{K_z} = \mathrm{diag}(k_{z1}, k_{z2}, \ldots; -k_{z1}, -k_{z2}, \ldots). \tag{25}$$

It has been proven that each column of matrix $\mathbf{T}$ consists of one eigenvector of $\mathbf{P}$, and $\pm k_{zm} (m = 1, 2, \ldots)$ are the eigenvalues of $\mathbf{P}$ and also the eigenvalues of the chiral media partially filled waveguide. If the transformed amplitude vector

$$\mathbf{A} = \mathbf{TB} = \begin{bmatrix} \mathbf{T_{11}} & \mathbf{T_{12}} \\ \mathbf{T_{21}} & \mathbf{T_{22}} \end{bmatrix} \mathbf{B} \tag{26}$$

is defined, an uncoupled wave equation system results as follows:

$$\frac{d\mathbf{B}}{dz} = -j\mathbf{K_z B}, \tag{27}$$

from which the amplitudes at a plane $z = w$ is obtained by

$$\mathbf{B}^{\pm}(w) = \mathbf{H}^{\pm}\mathbf{B}^{\pm}(0) \tag{28}$$

where

$$\mathbf{H}^{\pm} = \mathrm{diag}\big(\exp(\mp jk_{zm}w)\big).$$

From (26) and (28), we obtain the following equation after some matrix manipulations:

$$\begin{bmatrix} \mathbf{A}^{-}(0) \\ \mathbf{A}^{+}(w) \end{bmatrix} = \mathbf{S} \begin{bmatrix} \mathbf{A}^{+}(0) \\ \mathbf{A}^{-}(w) \end{bmatrix}. \tag{29}$$

where $\mathbf{S}$ is the multimode scattering matrix of the chiral media partially filled waveguide with length w. It is given by

$$\mathbf{S} = \begin{bmatrix} \mathbf{S_{11}} & \mathbf{S_{12}} \\ \mathbf{S_{21}} & \mathbf{S_{22}} \end{bmatrix} = \begin{bmatrix} \mathbf{T_{21}} & \mathbf{T_{22}}(\mathbf{H}^{-})^{-1} \\ \mathbf{T_{11}}\mathbf{H}^{+} & \mathbf{T_{12}} \end{bmatrix} \cdot \begin{bmatrix} \mathbf{T_{11}} & \mathbf{T_{12}}(\mathbf{H}^{-})^{-1} \\ \mathbf{T_{21}}\mathbf{H}^{+} & \mathbf{T_{22}} \end{bmatrix}^{-1}. \tag{30}$$

III. Numerical Results

In order to check the validity of the present approach, we first analyze a 2-D problem. We investigate the scattering of the TEM mode in a coaxial waveguide partially filled with chiral media, as shown in Fig. 2. The problem has already been analyzed by one of our authors using the mode-matching method [13]. We choose a typical 50-Ω coaxial waveguide with inner radius $a = 3.04$ mm and outer radius $b = 7.00$ mm. The frequency is taken to be 10 GHz so that only the dominant TEM mode can propagate in the hollow coaxial waveguide. The

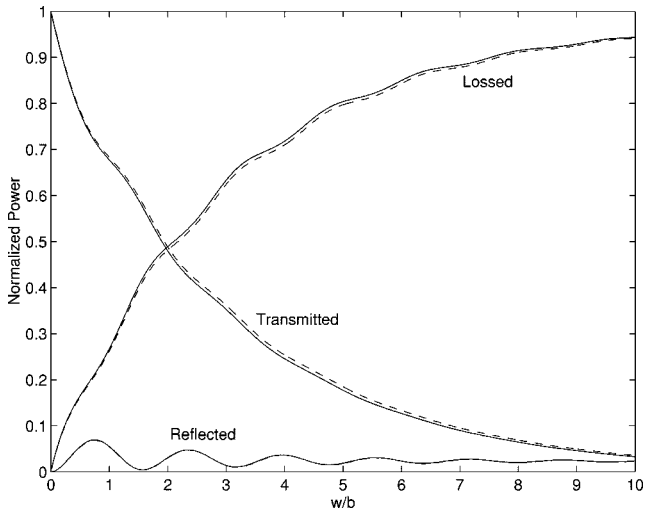

Fig. 3. Normalized reflected, transmitted, and lossed power of the TEM mode for the structure of Fig. 2 versus w/b. The solid lines are obtained by the coupled-mode method, while the dashed lines are obtained by the mode-matching method [13].

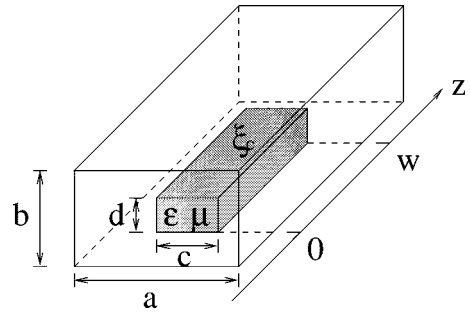

Fig. 4. Configuration of a rectangular waveguide partially filled with chiral media.

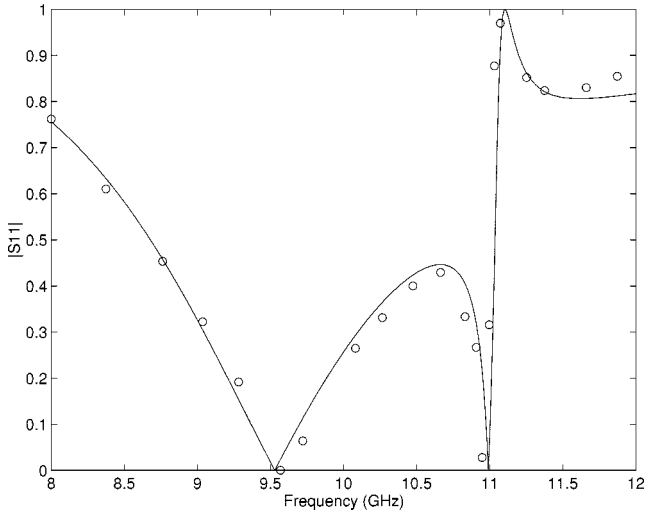

Fig. 5. Amplitude of reflection coefficient S_{11} versus frequency for a dielectric partially filled rectangular waveguide. Here, we take $a = 22.86$ mm, $c = 12$ mm, $b = d = 10.16$ mm, $\epsilon = 8.2\epsilon_0$, $\mu = \mu_0$, and $\xi_c = 0$, as shown in Fig. 1. The calculated results (solid line) are compared with measurements ("o") given in [25] and excellent agreement is found.

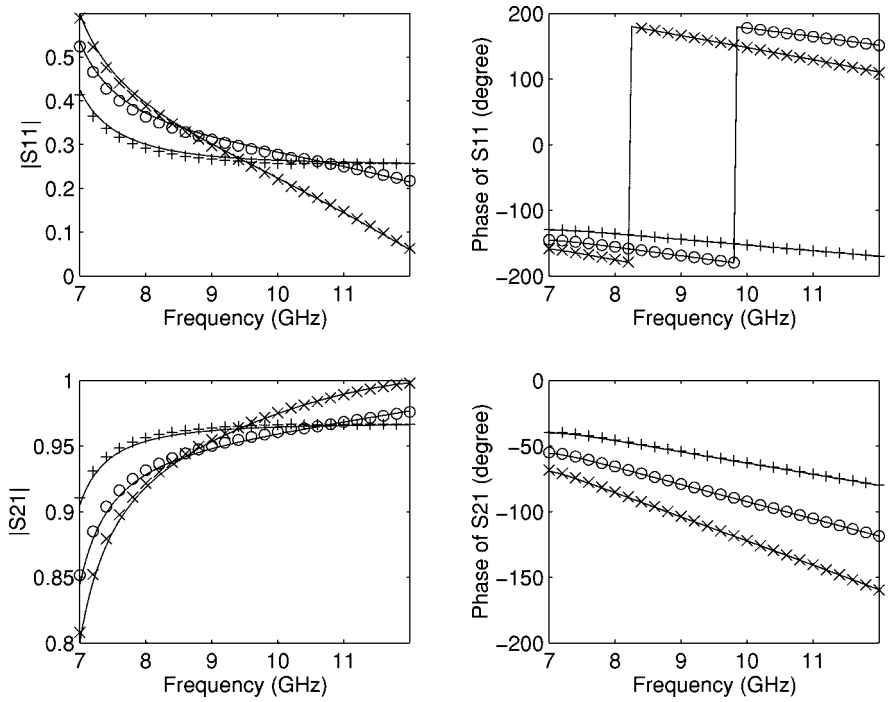

Fig. 6. Comparison of the results by the multimode mode-matching method with those obtained by the mode-matching method for achiral dielectric material partially filled rectangular waveguide. Here, we take $a = 22.86$ mm, $b = 10.16$ mm, $c = 11$ mm, $d = 5$ mm, $\epsilon = 2.5\epsilon_0$, and $\mu = \mu_0$, as shown in Fig. 4. The results obtained by the mode-matching method are depicted by "x," "o," and "+" for $w = 10, 7.5,$ and 5 mm, respectively; while the results obtained by the coupled-mode method are depicted by solid lines. Excellent agreement is found.

chiral material is taken to be lossy material with parameters $\epsilon_c = (2.1 - j0.5)\epsilon_0$, $\mu = \mu_0$, and $\kappa = 0.1$. We are interested in the reflected, transmitted, and lossed power as a function of the normalized length of the chiral media w/b. We observe from Fig. 3 that the reflected power oscillates with a decaying amplitude, the transmitted power drops down, and the lossed power increases as w/b increases due to material loss. In this figure, the solid lines provide the results of the present method, while the dashed lines depict the results of the mode-matching method [13]. Excellent agreements of the two methods are found, which validates this new approach.

Next, we use our program to analyze achiral dielectric material ($\xi_c = 0$) partially filled rectangular waveguide, as shown in Fig. 4. We consider a WR 75 waveguide with a width of $a = 22.86$ mm and a height of $b = 10.16$ mm. When this waveguide is operated in the 8–12-GHz frequency range, only the dominant H_{10} mode can propagate and all the higher order modes are evanescent. The inserted material slab has dimensions $c = 12$ mm, $d = b = 10.16$ mm, $w = 6$ mm, and dielectric constant $\epsilon = 8.2\epsilon_0$. In Fig. 5, the solid curve shows our calculations of the amplitude of input reflection coefficient $|S_{11}|$ versus frequency and is compared with measurements [25] and excellent agreement is found. Fig. 6 gives another example for comparing our results with those obtained by the mode-matching method proposed by one of the authors of [26]. Here, we take $a = 22.86$ mm, $b = 10.16$ mm, $c = 11$ mm, $d = 5$ mm, $\epsilon = 2.5\epsilon_0$, and $\mu = \mu_0$. The results obtained by the mode-matching method are depicted by "x," "o," and "+" for $w = 10, 7.5,$ and 5 mm, respectively, while the results obtained by the coupled-mode method are depicted by solid lines. We compare in this example not only amplitudes of the scattering parameters, but also phases of scattering parameters. We find excellent agreement for both amplitudes and phases. The above comparisons of our present results with experimental data and results by the mode-matching method for achiral case provide partial validation of our numerical method and implementation.

To investigate the effects of chirality admittance on the scattering properties of chiral media partially filled rectangular waveguide, we consider the WR 75 waveguide and fix the frequency at 9 GHz. We consider a sample of chiral media with a cross section of $c = 11$ mm by $d = 5$ mm in the middle of the waveguide and calculate the scattering parameters versus w, as shown in Fig. 4. In Fig. 7, the solid, dashed, dotted, and dotted–dashed lines give the results for the chirality admittance $\xi_c = 0$ (achiral case), 0.0005, 0.001, and 0.0015 mho cases, respectively. When the chirality admittance ξ_c is small, the difference between the RCP wavenumber k_+ and LCP wavenumber k_- in chiral media is small, and we find the influence of the chirality admittance is very weak. The difference between the curves for the achiral case (solid lines) and for $\xi_c = 0.0005$ mho is very small. This coincides with the qualitative analysis of Saadoun and Engheta [28] in that the influence of chirality admittance is a second order effect when the chirality admittance is small.

However, as the chirality admittance ξ_c increases, the difference between the RCP wavenumber k_+ and LCP wavenumber k_- in chiral media becomes larger and the influence of chirality admittance becomes larger. Moreover, we find the scattering parameters will become more sensitive to the increase of chirality admittance. For an example, we find the difference between the curves for $\xi_c = 0.001$ mho and for $\xi_c = 0.0005$ mho (where the difference of ξ_c is 0.0005 mho) is more evident

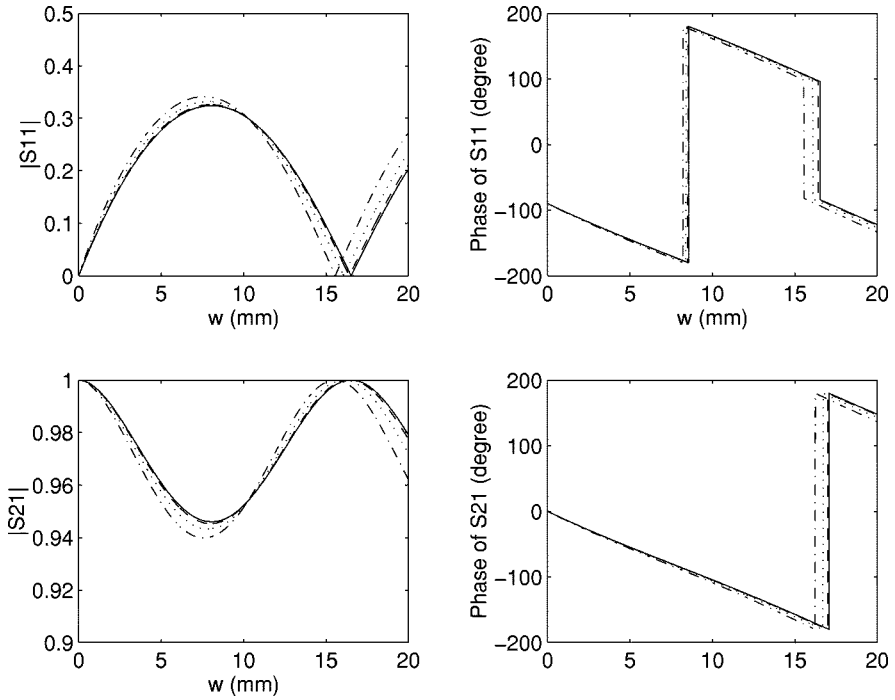

Fig. 7. Influence of small chirality admittance ξ_c on scattering parameters for a rectangular waveguide partially filled case. Here, we show the amplitudes and phases of reflection coefficient S_{11} and transmission coefficient S_{21} versus the length w of chiral media at a fixed frequency of 9 GHz. We take $a = 22.86$ mm, $b = 10.16$ mm, $c = 11$ mm, $d = 5$ mm, $\epsilon = 2.5\epsilon_0$, and $\mu = \mu_0$, as shown in Fig. 4. The solid, dashed, dotted, and dotted–dashed line give the cases for chirality admittance. ξ_c takes the value of 0 (achiral case), 0.0005, 0.001, and 0.0015 mho, respectively.

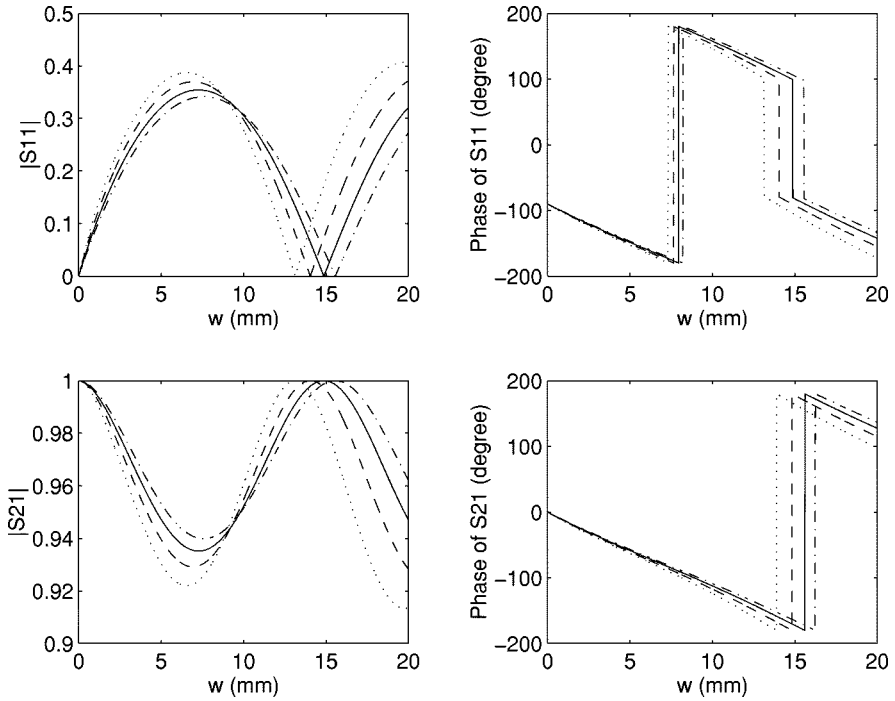

Fig. 8. Influence of large chirality admittance ξ_c on scattering parameters for a rectangular waveguide partially filled case. Here, we show the amplitudes and phases of reflection coefficient S_{11} and transmission coefficient S_{21} versus the length w of chiral media at a fixed frequency of 9 GHz. We take $a = 22.86$ mm, $b = 10.16$ mm, $c = 11$ mm, $d = 5$ mm, $\epsilon = 2.5\epsilon_0$, and $\mu = \mu_0$, as shown in Fig. 4. The dotted–dashed line, solid line, dashed line, and dotted line give the cases for chirality admittance. ξ_c takes the value of 0.0015 (achiral case), 0.002, 0.0025, and 0.003 mho, respectively.

than the difference between the curves for $\xi_c = 0.0015$ mho and for $\xi_c = 0.001$ mho (where the difference of ξ_c is also 0.0005 mho). This effect is more clearly depicted in Fig. 8 for large values of chirality admittance. In Fig. 8, we give the results when the chirality admittance is 0.0015 mho (dotted–dashed lines), 0.002 mho (solid lines), 0.0025 mho (dashed lines), and 0.003 mho (dotted lines). We find the difference between the curves for $\xi_c = 0.0025$ mho and $\xi_c = 0.003$ mho is the largest compared with the difference between any two other adjacent curves. A simple physical explanation can be made by

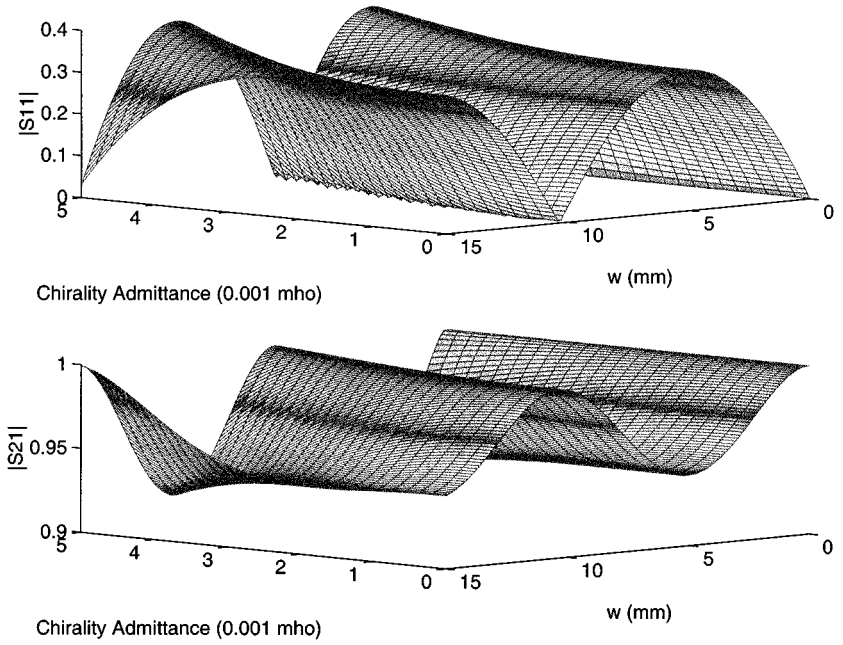

Fig. 9. Influence of chirality admittance ξ_c on the amplitudes of scattering parameters for coaxial waveguide partially filled case. Here, we show the amplitudes of reflection coefficient S_{11} and transmission coefficient S_{21} versus the length w of chiral media and chirality admittance ξ_c at a fixed frequency of 10 GHz for coaxial waveguide, as shown in Fig. 2. We take $a = 3.04$ mm, $b = 7.0$ mm, $c = 6.0$ mm, $\epsilon = 2.5\epsilon_0$, and $\mu = \mu_0$.

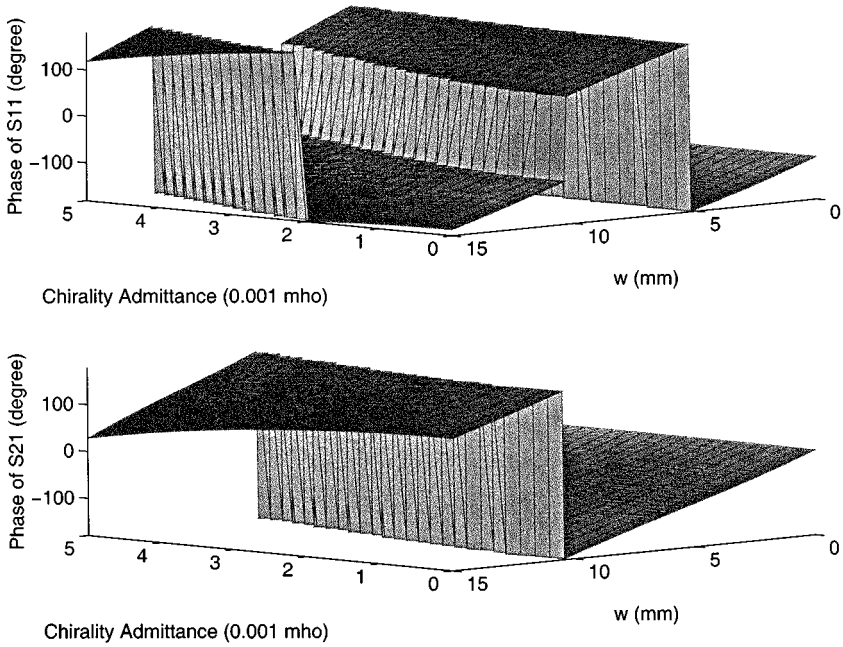

Fig. 10. Influence of chirality admittance ξ_c on the phases of scattering parameters for a coaxial waveguide partially filled case. Here, we show the phases of reflection coefficient S_{11} and transmission coefficient S_{21} versus the length w of chiral media and chirality admittance ξ_c at a fixed frequency of 10 GHz for a coaxial waveguide, as shown in Fig. 2. We take $a = 3.04$ mm, $b = 7.0$ mm, $c = 6.0$ mm, $\epsilon = 2.5\epsilon_0$, and $\mu = \mu_0$.

considering (3), from which we find the sensitivity of $k_\pm$ to ξ_c given by

$$S_{\xi_c}^{k_\pm} = \frac{dk_\pm/k_\pm}{d\xi_c/\xi_c} = \pm\frac{1}{\sqrt{\frac{\epsilon}{\mu\xi_c^2}+1}} = \pm\xi_c\sqrt{\frac{\mu}{\epsilon_c}} = \pm\kappa. \quad (31)$$

From (31), we find $|S_{\xi_c}^{k_\pm}|$ does not keep a constant value, but increases as ξ_c increases. This means that the sensitivity of $k_\pm$ and, therefore, the scattering parameters to ξ_c is large for ξ_c large and small for ξ_c small. Also, when ξ_c tends to be zero, the sensitivity tends to be zero, as shown in Fig. 8.

We further investigate the effects of chirality admittance for a coaxial waveguide. Here, we choose the same coaxial waveguide as that in Fig. 3. The radius c of chiral material is taken to be 6 mm and the material parameters are taken to be $\epsilon = 2.5\epsilon_0$ and $\mu = \mu_0$. The results in a 3-D surface graph have been given in Figs. 9 and 10. The same property that the sensitivity of the scattering parameters to chirality admittance increases as the

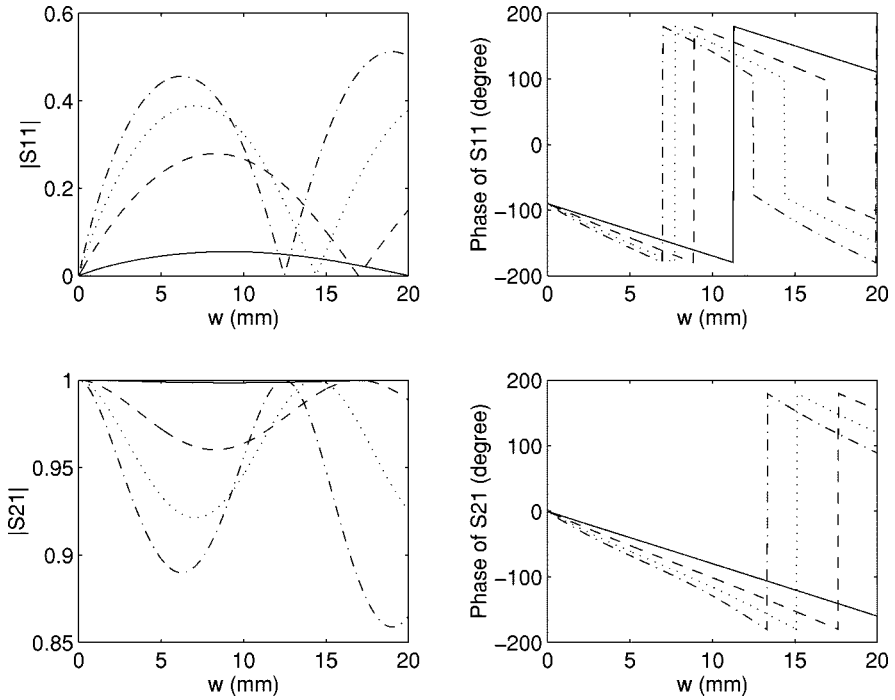

Fig. 11. Influence of dielectric constant on scattering parameters for a rectangular waveguide partially filled case. Here, we show the amplitudes and phases of reflection coefficient S_{11} and transmission coefficient S_{21} versus the length w of chiral media at a fixed frequency of 9 GHz. Here, we take $a = 22.86$ mm, $b = 10.16$ mm, $c = 11$ mm, $d = 5$ mm, $\xi_c = 0.0001$ mho, and $\mu = \mu_0$, as shown in Fig. 4. The dotted–dashed, solid, dashed, and dotted line give the cases for dielectric constant. ϵ takes the value of ϵ_0, $2\epsilon_0$, $3\epsilon_0$, and $4\epsilon_0$, respectively.

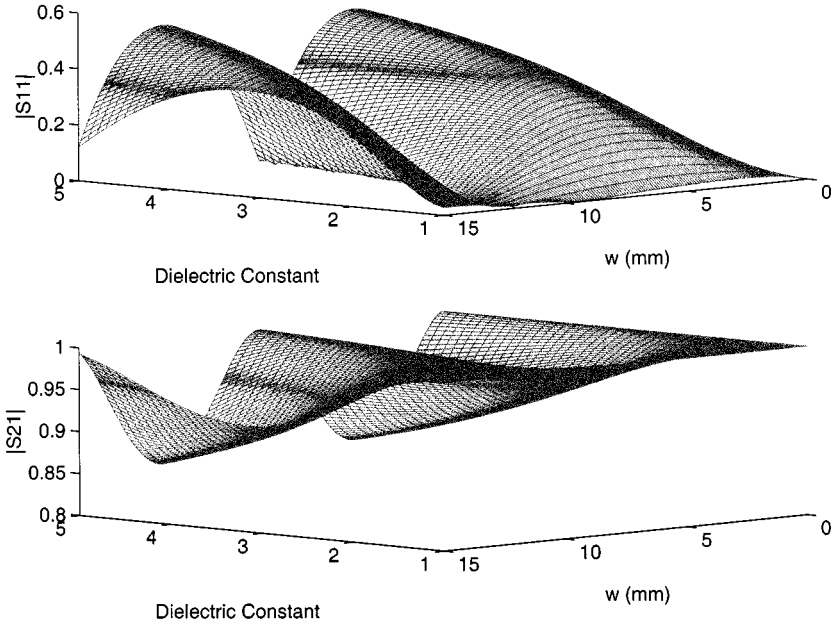

Fig. 12. Influence of dielectric constant on the amplitudes of scattering parameters for a coaxial waveguide partially filled case. Here, we show the amplitudes of reflection coefficient S_{11} and transmission coefficient S_{21} versus the length w of chiral media and dielectric constant ϵ at a fixed frequency of 10 GHz. We take $a = 3.04$ mm, $b = 7.0$ mm, $c = 6.0$ mm, $\xi_c = 0.0001$ mho, and $\mu = \mu_0$, as shown in Fig. 2.

chirality admittance increases has been shown clearly in these figures.

In Fig. 11, we investigate how the dielectric constant affects the propagation properties of a chiral media partially filled rectangular waveguide. Here, we choose the WR 75 waveguide operating at 9 GHz and fix the chirality admittance $\xi_c = 0.0015$ mho and $\mu = \mu_0$. We consider a sample of chiral media with a cross section of $c = 11$ mm by $d = 5$ mm in the middle of the waveguide and calculate the scattering parameters versus w, as shown in Fig. 4. In Fig. 11, the solid, dashed, dotted, and dotted–dashed lines give the results for the dielectric constant of $\epsilon = \epsilon_0$, $\epsilon = 2\epsilon_0$, $\epsilon = 3\epsilon_0$, and $\epsilon = 4\epsilon_0$, respectively. Here, we find the influence of dielectric constant is quite significant, which verifies that the influence of dielectric constant is a first-order effect as the perturbation theory indicates. This may also be explained from the fact that

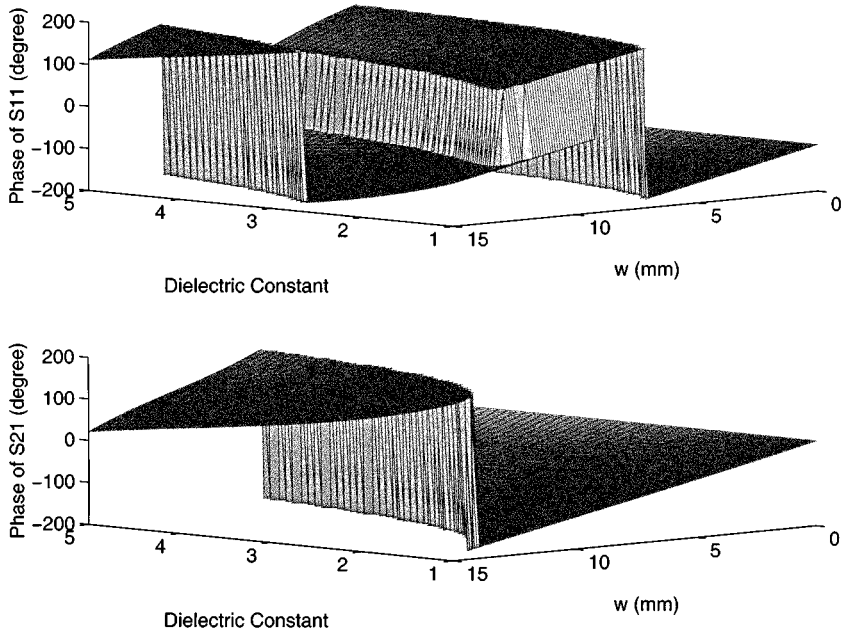

Fig. 13. Influence of dielectric constant on the phases of scattering parameters for a coaxial waveguide partially filled case. Here, we show the phases of reflection coefficient S_{11} and transmission coefficient S_{21} versus the length w of chiral media and dielectric constant ϵ at a fixed frequency of 10 GHz. We take $a = 3.04$ mm, $b = 7.0$ mm, $c = 6.0$ mm, $\xi_c = 0.0001$ mho, and $\mu = \mu_0$, as shown in Fig. 2.

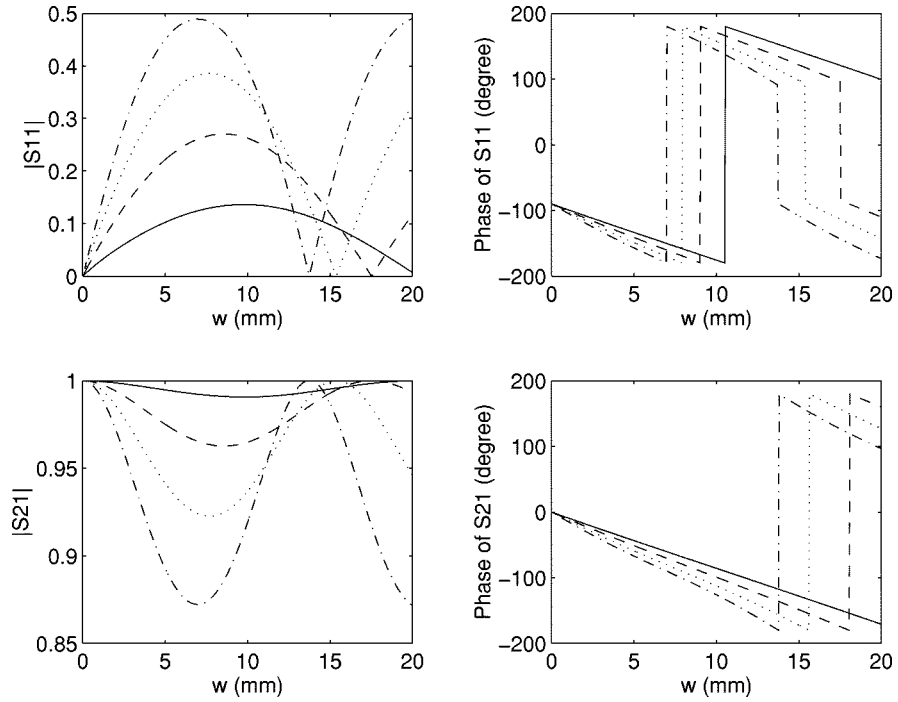

Fig. 14. Influence of the height of chiral media on scattering parameters for a rectangular waveguide partially filled case. Here, we show the amplitudes and phases of reflection coefficient S_{11} and transmission coefficient S_{21} versus the length w of chiral media at a fixed frequency of 9 GHz. We take $a = 22.86$ mm, $b = 10.16$ mm, $c = 11$ mm, $\epsilon = 2\epsilon_0$ $\xi_c = 0.0001$ mho, and $\mu = \mu_0$, as shown in Fig. 4. The dotted–dashed, solid, dashed, and dotted line give the cases for dielectric constant. ϵ takes the value of $d = b/4, b/2, 3b/4$, and b, respectively.

when ξ_c is small, the sensitivity of $k_\pm$ to the dielectric constant is almost a constant value of 0.5 no matter what value the dielectric constant ϵ takes. For the coaxial waveguide case, the same properties may be found from the 3-D surface plot shown in Figs. 12 and 13.

The influence of the height d of the chiral material to the scattering properties for a chiral media partially filled rectangular waveguide is investigated in Fig. 14. Here, we fix the width of the chiral material to be $c = 11$ mm and change the height d in Fig. 4. The solid, dashed, dotted, and dotted–dashed line depict the case when $d = b/4, b/2, 3b/4$, and b, respectively. It is found from the figure that the influence of the height d is significant and the influence is always large no matter if d is small (d tends to be zero) or large (d tends to be b). The reason is that for

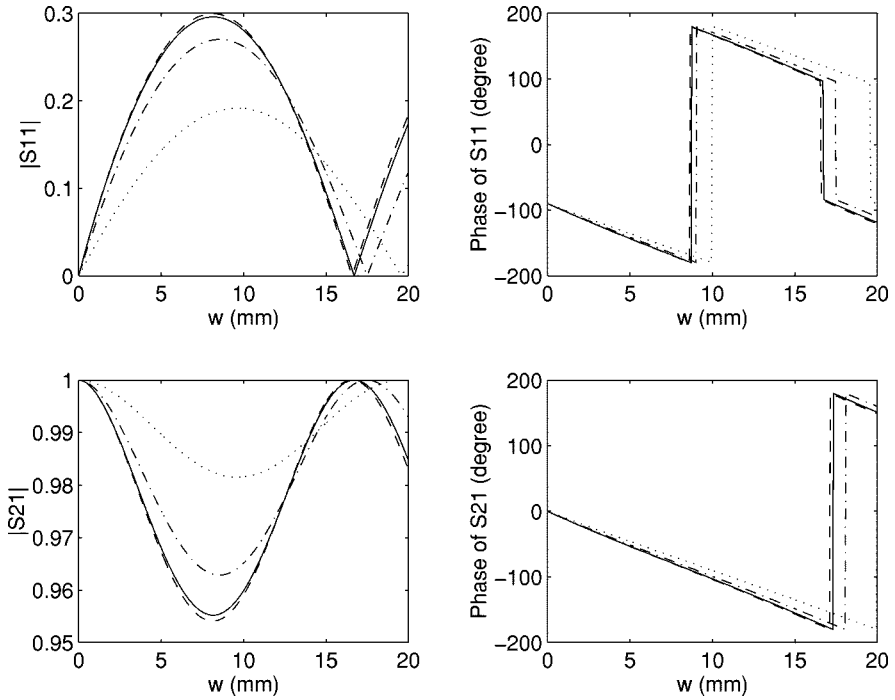

Fig. 15. Influence of the width of chiral media on scattering parameters for a rectangular waveguide partially filled case. Here, we show the amplitudes and phases of reflection coefficient S_{11} and transmission coefficient S_{21} versus the length w of chiral media at a fixed frequency of 9 GHz. We take $a = 22.86$ mm, $b = 10.16$ mm, $d = 5$ mm, $\epsilon = 2\epsilon_0$ $\xi_c = 0.0001$ mho, and $\mu = \mu_0$, as shown in Fig. 4. The dotted–dashed, solid, dashed, and dotted line give the cases for dielectric constant. ϵ takes the value of $c = a/4$, $a/2$, $3a/4$, and a, respectively.

the incident H_{10} mode, the strongest electric field occurs in the middle of the width of the waveguide. The increase of the height gives the incident mode strong disturbance. It is also interesting to note that the influence of the width c of the chiral material is quite different from the influence of height d. In Fig. 15, we fix $d = 5$ mm and show the cases for $c = a/4$, $a/2$, $3a/4$, and a with a dotted, dotted–dashed, solid, and dashed line, respectively. It is clear that when c is small, the influence of c is strong because the electric field of the incident mode in the middle of the width is the strongest. The influence of c is gradually decreased when c is further increased because the electric field of the incident mode decreases for the increased part of c (which is zero at the boundary). The curves for $c = 3a/4$ (solid lines) are found to be very close to those for $c = a$ (dashed lines).

IV. Conclusion

We have reported a comprehensive study of discontinuities in chirowaveguides. To our knowledge, this is also the first study of the 3-D discontinuity problem in chirowaveguides. The scattering characteristics of a metallic waveguide partially filled with chiral media are carefully investigated by a multimode coupled-mode method. Rather than taking the two-mode approximation typical of the traditional coupled-mode theory, we diagonalize the coupling matrix and take into account the contribution of higher order modes. This is used to find the multimode scattering matrix for the discontinuity. We have shown that the multimode coupled-mode method can be effectively used as a numerical method for this kind of discontinuity problems.

To check the validity of our method, we have first analyzed a coaxial waveguide partially filled with lossy chiral media. Our results are compared with those obtained by the mode-matching method and excellent agreement is found. We have also checked our results for an achiral dielectric material partially filled rectangular waveguide, and excellent agreement between our calculation and experimental data, as well as data from the mode-matching method is again found. Based upon our analysis, we have numerically calculated the scattering parameters for chiral media partially filled rectangular waveguide and coaxial waveguide. We investigate the effects of chirality admittance on scattering properties and find the sensitivity of the scattering parameters to chirality admittance increases as the chirality admittance increases. The effect of the dielectric constant is also investigated and it is found to have a great influence. We have also discussed the effects of the height and width of chiral media for a rectangular waveguide case. We find the influence of the height is always large, but the influence of the width decreases as the width increases. Our results have been explained by underlying physical insights.

It is noted that chirowaveguide discontinuity analysis is important for the application to develop useful devices, such as directional couplers, filters, mode converters, etc. Research on these topics are in progress.

References

[1] D. L. Jaggard, A. R. Mickelson, and C. H. Papas, "On electromagnetic waves in chiral media," *Appl. Phys.*, vol. 18, pp. 211–216, 1979.

[2] D. L. Jaggard and N. Engheta, "Chirality in electrodynamics: Modeling and applications," in *Directions in Electromagnetic Wave Modeling*, H. L. Bertoni and L. B. Felson, Eds. New York: Plenum, 1991, pp. 435–446.

[3] H. N. Kritikos, N. Engheta, and D. L. Jaggard, "Symmetry in material media," in *Symmetry in Electromagnetics*, C. Baum and H. N. Kritikos, Eds. New York: Taylor & Francis, 1995, ch. 4.

[4] N. Engheta and P. Pelet, "Modes in chirowaveguides," *Opt. Lett.*, vol. 14, pp. 593–595, 1989.
[5] P. Pelet and N. Engheta, "The theory of chirowaveguides," *IEEE Trans. Antennas Propagat.*, vol. 38, pp. 90–98, Jan. 1990.
[6] F. Mariotte, P. Pelet, and N. Engheta, "A review of recent study of guided waves in chiral media," in *Bianisotropic and Bi-isotropic Media and Applications*, A. Priou, Ed. Cambridge, MA: EMW, 1994, PIER 9, pp. 311–350.
[7] P. Pelet and N. Engheta, "Modal analysis of rectangular chirowaveguides with metallic walls using the finite-difference method," *J. Electromagnetic Waves Applicat.*, vol. 6, pp. 1277–1285, 1992.
[8] K. Flood and D. L. Jaggard, "Single-mode operation in symmetric planar waveguides using isotropic chiral media," *Opt. Lett.*, vol. 21, pp. 474–476, 1996.
[9] C. R. Paiva and A. M. Barbosa, "A linear-operator formalism for the analysis of inhomogeneous biisotropic planar waveguides," *IEEE Trans. Microwave Theory Tech.*, vol. 40, pp. 672–678, Apr. 1993.
[10] C. R. Paiva, A. L. Topa, and A. M. Barbosa, "Semileaky waves in dielectric chirowaveguides," *Opt. Lett.*, vol. 17, pp. 1670–1672, Dec. 1992.
[11] F. Mariotte and N. Engheta, "Reflection and transmission of guided electromagnetic waves at an air–chiral interface and at a chiral slab in a parallel-plate waveguide," *IEEE Trans. Microwave Theory Tech.*, vol. 41, pp. 1895–1906, Nov. 1993.
[12] ——, "Reflection from a lossy chiral slab (with and without metallic backing) in a parallel plate waveguide," *Radio Sci.*, vol. 30, pp. 827–834, 1995.
[13] X. Wu and F. Mariotte, "Equivalent network analysis of the scattering of TEM wave in coaxial waveguide partially filled with chiral media," in *Proc. Asia–Pacific Microwave Conf.*, Taejon, Korea, 1995.
[14] G. Busse and A. F. Jacob, "Lossy chiral slabs in circular waveguides," *Proc. Inst. Elect. Eng.*, pt. H, vol. 143, pp. 51–56, 1996.
[15] X. Wu and D. L. Jaggard, "Planar chirowaveguide with discontinuities," *Microwave Opt. Technol. Lett.*, vol. 10, pp. 280–284, 1997.
[16] ——, "Discontinuities in planar chirowaveguides," *IEEE Trans. Microwave Theory Tech.*, vol. 45, pp. 640–647, May 1997.
[17] P. Pelet and N. Engheta, "Coupled-mode theory for chirowaveguides," *J. Appl. Phys.*, vol. 67, pp. 2742–2745, 1990.
[18] J. Mazur, "Nonreciprocal phenomena in coupled guides filled with chiroferrite media," *J. Electromagnetic Waves Applicat.*, vol. 7, pp. 1395–1415, 1993.
[19] H. Cory and T. Tamir, "Coupling processes in circular open chirowaveguides," *Proc. Inst. Elect. Eng.*, pt. H, vol. 139, pp. 165–170, 1992.
[20] D. L. Jaggard, N. Engheta, M. W. Kowarz, P. Pelet, J. C. Liu, and Y. Kim, "Periodic chiral structures," *IEEE Trans. Antennas Propagat.*, vol. 37, pp. 1447–1452, Nov. 1989.
[21] K. M. Flood and D. L. Jaggard, "Distributed feedback lasers in chiral media," *IEEE J. Quantum Electron.*, vol. 30, pp. 339–345, Feb. 1994.
[22] ——, "Bandgap structure for periodic chiral media," *J. Opt. Soc. Amer. A, Opt. Image Sci.*, vol. 13, pp. 1395–1406, 1996.
[23] Y. Xu and R. G. Bosisio, "An efficient method for study of general bi-anisotropic waveguides," *IEEE Trans. Microwave Theory Tech.*, vol. 43, pp. 873–879, Apr. 1995.
[24] ——, "A study on the solutions of chirowaveguides and bianisotropic waveguides with the use of coupled-mode analysis," *Microwave Opt. Technol. Lett.*, vol. 14, pp. 308–311, 1997.
[25] H. Chaloupka, "A coupled-line model for the scattering by dielectric and ferromagnetic obstacles in waveguides," *Arch. Elektron. Uebertrag.*, vol. 34, pp. 145–151, 1990.
[26] X. Wu and S. Xu, "Dielectric waveguide 3-D discontinuities," *Int. J. Infrared Millim. Waves*, vol. 16, no. 4, pp. 839–861, 1995.
[27] R. E. Collin, *Field Theory of Guided Waves*, 2nd ed. New York: IEEE Press, 1991, ch. 5.
[28] M. M. Saadoun and N. Engheta, "Theoretical study of variation of propagation constant in a cylindrical Waveguide due to chirality: Chiro-phase shifting," *IEEE Trans. Microwave Theory Tech.*, vol. 42, pp. 1690–1694, Sept. 1994.

Thomas X. Wu (S'97–M'99–SM'02) received the B.S.E.E. and M.S.E.E. degrees from the University of Science and Technology of China (USTC), Hefei, China, in 1988 and 1991, respectively, and the M.S. and Ph.D. degrees in electrical engineering from the University of Pennsylvania, Philadelphia, in 1997 and 1999, respectively.

From 1991 to 1995, he was with the faculty of the Department of Electrical Engineering and Information Science, USTC, as an Assistant and Lecturer. In Fall 1999, he joined the School of Electrical Engineering and Computer Science (SEECS), University of Central Florida (UCF), Orlando, as an Assistant Professor. He is the Director of the High Speed Electronics and Systems Laboratory, UCF. He also has secondary appointments at the Applied Materials Processing and Applications Center (AMPAC), Florida Space Institute (FSI), and Nano-Technology Research Center, UCF. He has authored or coauthored over 20 journal and 40 conference publications. He has also reviewed papers for several important technical journals. His current research interests and projects include CMOS/BiCMOS RF integrated circuits (RFICs), meta-material, liquid crystal devices, high-speed miniaturized motor, electronic packaging of RF surface acoustic wave (SAW) devices, chaotic electromagnetics, and high-speed CODEC design. He is listed in *Who's Who in Science and Engineering*, *Who's Who in America*, and *Who's Who in the World*.

Dr. Wu was the recipient of the 1991 Prize of the President of the Chinese Academy of Sciences.

Dwight L. Jaggard (S'68–M'77–SM'86–F'91) received the B.S.E.E. and M.S.E.E. degrees from the University of Wisconsin–Madison, in 1971 and 1972, respectively, and the Ph.D. degree in electrical engineering and applied physics from the California Institute of Technology, Pasadena, in 1976.

Since 1980, he has performed research in electromagnetics and optics with an emphasis on waves and complex media and methods of inverse scattering and imaging at the Moore School of Electrical Engineering, University of Pennsylvania, Philadelphia, where he is currently a Professor of electrical engineering and co-founder of the Complex Media Laboratory. He co-edited and was a contributor to *Recent Advances in Electromagnetic Theory* (Berlin, Germany: Springer-Verlag, 1990) and was contributor to *Symmetry in Electromagnetics* (New York: Taylor & Francis, 1995), *Fractals in Engineering*, (Berlin, Germany: Springer-Verlag, 1997), *Fractals: Theory and Applications in Engineering* (Berlin, Germany: Springer-Verlag, 1999), and *Frontiers of Electromagnetics* (Piscataway, NJ: IEEE Press, 2001). He has also served as a consultant to government and industry. He has served as an Editor of the *Journal of Electromagnetic Wave Applications* and Editor of several special sections of the *Journal of the Optical Society*. His current research involves the fundamentals and applications of fractal electrodynamics, electromagnetic chirality, and the effects of symmetry and topology on waves in knotted media.

Prof. Jaggard is a Fellow of the Optical Society of America since 1995. He has served as an editor for the PROCEEDINGS OF THE IEEE. He was a member of the Editorial Board of the PROCEEDINGS OF THE IEEE. He was an associate editor of the IEEE TRANSACTIONS ON ANTENNAS AND PROPAGATION. He was the recipient of the S. Reid Warren Award for Distinguished Teaching and the Christian F. and Mary R. Lindback Award for Distinguished Teaching.